Linear and nonlinear optical responses influenced by broken symmetry in an array of gold nanoparticles

Brian K. Canfield[1], Sami Kujala[1], Konstantins Jefimovs[2], Jari Turunen[2], and Martti Kauranen[1]

[1]*Institute of Physics, Optics Laboratory, Tampere University of Technology P. O. Box 692 FI-33101 Tampere, Finland*

[2]*Department of Physics, University of Joensuu P. O. Box 111 FI-80101 Joensuu, Finland*

brian.canfield@tut.fi

Abstract: An array of low-symmetry, L-shaped gold nanoparticles is shown to exhibit high sensitivity to the state of incident polarization. Small imperfections in the shape of the actual particles, including asymmetric arm lengths and edge distortions, break the symmetry attributed to an ideal particle. This broken symmetry leads to a large angular displacement of the extinction axes from their expected locations. More significantly, second-harmonic generation experiments reveal significant second-order susceptibility tensor components forbidden to the ideal symmetry.

OCIS codes: (260.5430) Polarization, (190.4720) Optical nonlinearities of condensed matter, (260.3910) Metals, optics of.

References and links

1. W. Gotschy, K. Vonmetz, A. Leitner, and F. R. Aussenegg, "Optical dichroism of lithographically designed silver nanoparticles," Opt. Lett. **21**, 1099–1101 (1996).
2. W. Gotschy, K. Vonmetz, A. Leitner, and F. R. Aussenegg, "Thin films by regular patterns of metal nanoparticles: tailoring the optical properties by nanodesign," Appl. Phys. B **63**, 381–384 (1996).
3. S. Linden, J. Kuhl, and H. Giessen, "Controlling the Interaction between Light and Gold Nanoparticles: Selective Suppression of Extinction," Phys. Rev. Lett. **86**, 4688–4691 (2001).
4. W. Rechberger, A. Hohenau, A. Leitner, J. R. Krenn, B. Lamprecht, and F. R. Aussenegg, "Optical properties of two interacting gold nanoparticles," Opt. Commun. **220**, 137–141 (2003).
5. K.-H. Su, Q.-H. Wei, X. Zhang, J. J. Mock, D. R. Smith, and S. Schultz, "Interparticle Coupling Effects on Plasmon Resonances of Nanogold Particles," Nano Lett. **3**, 1087–1090 (2003).
6. J. Aizpurua, P. Hanarp, D. S. Sutherland, M. Käll, G. W. Bryant, and F. J. G. d. Abajo, "Optical properties of gold nanorings," Phys. Rev. Lett. **90**, 057401 (2003).
7. C. L. Haynes, A. D. McFarland, L. L. Zhao, R. P. V. Duyne, G. C. Schatz, L. Gunnarsson, J. Prikulis, B. Kasemo, and M. Käll, "Nanoparticle Optics: The Importance of Radiative Dipole Coupling in Two-Dimensional Nanoparticle Arrays," J. Phys. Chem. B **107**, 7337–7342 (2003).
8. G. Schider, J. R. Krenn, A. Hohenau, H. Ditlbacher, A. Leitner, F. R. Aussenegg, W. L. Schaich, I. Puscasu, B. Monacelli, and G. Boreman, "Plasmon dispersion relation of Au and Ag nanowires," Phys. Rev. B **68**, 155427 (2003).
9. T. Vallius, K. Jefimovs, J. Turunen, P. Vahimaa, and Y. Svirko, "Optical activity in subwavelength-period arrays of chiral metallic particles," Appl. Phys. Lett. **83**, 234–236 (2003).
10. A. Papakostas, A. Potts, D. M. Bagnall, S. L. Prosvirnin, H. J. Coles, and N. I. Zheludev, "Optical Manifestations of Planar Chirality," Phys. Rev. Lett. **90**, 107404 (2003).
11. B. Lamprecht, A. Leitner, and F. R. Aussenegg, "SHG studies of plasmon dephasing in nanoparticles," Appl. Phys. B **68**, 419–423 (1999).

#5420 - $15.00 US Received 1 October 2004; revised 19 October 2004; accepted 20 October 2004

12. H. Tuovinen, M. Kauranen, K. Jefimovs, P. Vahimaa, T. Vallius, and J. Turunen, "Linear and second-order nonlinear optical properties of arrays of noncentrosymmetric gold nanoparticles," J. Nonlinear Opt. Phys. **11**, 421–432 (2002).
13. V. M. Shalaev and A. K. Sarychev, "Nonlinear optics of random metal-dielectric films," Phys. Rev. B **57**, 13,265–13,288 (1998).
14. M. I. Stockman, D. J. Bergman, C. Anceau, S. Brasselet, and J. Zyss, "Enhanced Second-Harmonic Generation by Metal Surfaces with Nanoscale Roughness: Nanoscale Dephasing, Depolarization, and Correlations," Phys. Rev. Lett. **92**, 057402 (2004).
15. A. K. Sarychev, V. A. Shubin, and V. M. Shalaev, "Anderson localization of surface plasmons and nonlinear optics of metal-dielectric composites," Phys. Rev. B **60**, 16,389–16,408 (1999).
16. K. Li, M. I. Stockman, and D. J. Bergman, "Self-Similar Chain of Metal Nanospheres as an Efficient Nanolens," Phys. Rev. Lett. **91**, 227402 (2003).
17. B. K. Canfield, S. Kujala, M. Kauranen, K. Jefimovs, T. Vallius, and J. Turunen, "Remarkable polarization sensitivity of gold nanoparticle arrays," submitted Sept. 2004 to Appl. Phys. Lett.
18. Y. R. Shen, *The Principles of Nonlinear Optics* (John Wiley & Sons, New York, 1984).
19. R. W. Boyd, *Nonlinear Optics* (Academic Press, San Diego, 1992).
20. M. Kauranen, T. Verbiest, and A. Persoons, "Second-order nonlinear optical signatures of surface chirality," J. Mod. Opt. **45**, 403–423 (1998).

1. Introduction

Investigation of the optical properties of metal nanoparticle arrays is proceeding with intense interest. Much work concerns highly symmetric ellipsoidal or cylindrical particles [1, 2, 3, 4, 5]. Several other geometries with lower-symmetry properties have recently been reported as well: rings [6], triangles [7], wires [8], and gammadion structures [9, 10]. Very low symmetry L-shaped particles have also been examined using both linear and nonlinear techniques [11, 12]. Only a few studies of polarization effects in nanoparticles, beyond well-known dichroism, have been reported, and research into nonlinear responses is sparse. Theoretical treatments have drawn attention to the importance of small-scale irregularities in metal nanostructures [13, 14]. Surface plasmons tend to converge around these irregularities, inducing 'hot spots' in the local field that can be several orders of magnitude greater than the exciting field [15]. Such local-field enhancement can then be used for nanoscale focusing [16] or to facilitate nonlinear interactions.

In this Article we present results of detailed linear and nonlinear polarization measurements on an array of low-symmetry, L-shaped gold nanoparticles. The optical response of the array is highly sensitive to the polarization state of the incident beam. The actual nanoparticles possess small shape deviations from the geometric ideal that break the array's symmetry and exert a substantial influence on its optical responses. Second-harmonic generation (SHG) measurements are especially sensitive to the lack of symmetry and therefore reveal intriguing polarization responses. In particular, new SH tensor components not allowed for ideal, symmetric particles are observed.

2. Sample and experimental apparatus

The gold nanoparticle array was fabricated using a Leica LION LV-1 electron-beam lithography (EBL) tool (beam energy 15 keV, beam current 90 pA, step size 5 nm) followed by standard development, deposition, and lift-off processes [12]. A bottom-up nanoparticle cross section consists of a glass substrate; a 2 nm Cr adhesion layer, which does not extend beyond the nanoparticle perimeter and aids in bonding the gold to the substrate; a 20 nm layer of gold; and a 20 nm layer of protective glass. The particle arms are nominally 190 nm long with 110 nm linewidth, and the array period is 400 nm. The array area covers $(600\,\mu\mathrm{m})^2$.

A natural choice of principal axes, denoted X and Y (top left, Fig. 1), is suggested by the symmetry of an ideal 'L' with equal arm lengths. The ideal array possesses a mirror plane along X. During fabrication, however, small shape distortions from ideal are introduced to the actual nanoparticles. Close scrutiny of the representative micrograph also reveals that the vertical arms

#5420 - $15.00 US Received 1 October 2004; revised 19 October 2004; accepted 20 October 2004

are about 5% longer than the horizontal arms, resulting from a slight astigmatism of the electron beam.

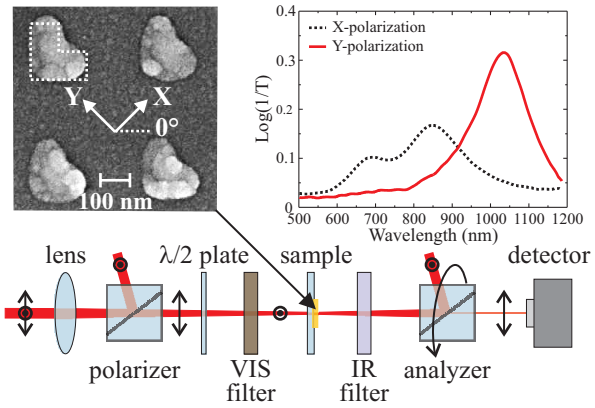

Fig. 1. Top left: scanning electron micrograph of the sample, indicating the coordinate system used. Top right: polarized extinction spectra. Bottom: basic experimental setup.

The extinction of the array for both principal polarizations was measured [17]. The array exhibits strong dichroism between the main X (853 nm) and Y (1030 nm) plasmon resonances, and extinction along Y is approximately twice as strong as along X (top right, Fig. 1).

Detailed analysis of the linear and nonlinear polarization responses as a function of the incident linear polarization direction, θ, were conducted using the general setup shown in Fig. 1. The laser beam (Time-Bandwidth GLX-200, central wavelength 1060 nm, pulse length 200 fs, repetition rate 82 MHz, average power 350 mW) was chopped (not shown) and moderately focused at normal incidence on the sample with a lens (focal length 20 cm). Precise incident polarization was controlled by a polarizer and a zero-order half-wave plate. The visible (VIS) and infrared (IR) blocking filters were used only for SHG measurements. For the transmission measurement, the analyzer was not used. In the linear measurements, the detector consisted of a scatter plate and a photodiode connected to a lock-in amplifier (also not shown), referenced to the chopper frequency. In the SHG measurements, the detector was a photomultiplier tube, again connected to the lock-in. Note that the Y-polarization plasmon peak is nearly resonant with the laser wavelength.

3. Results and discussion

The transmission curve (referenced to substrate-only transmission) shown in Fig. 2(a) exhibits a considerable angular shift, α, of the primary extinction axes from the expected axes X (45 °) and Y (135°). We determined the location of these new axes, A and B, by fitting the transmission data to [17]

$$T = T_A \sin^2(\theta - 45^\circ - \alpha) + T_B \cos^2(\theta - 45^\circ - \alpha), \tag{1}$$

where T_A and T_B are the transmittances along axes A and B, respectively. (The factor of 45 ° relates the sample to the EBL writing frame for experimentally expedient alignment.) The fitted angular shift is $\alpha = -7.6^\circ \pm 0.1^\circ$. This shift is much larger than expected based only on the difference in arm lengths.

Consider a particle with its vertical arm a factor ρ longer than its horizontal arm (length L, Fig. 3). The axis angle, ϕ, is determined from $\phi = \arctan(\rho)$. For equal arm lengths, $\rho = 1$ and $\phi = 45^\circ$, matching the X-Y axes. For larger values of ρ, the axes will be shifted from X and

#5420 - $15.00 US Received 1 October 2004; revised 19 October 2004; accepted 20 October 2004

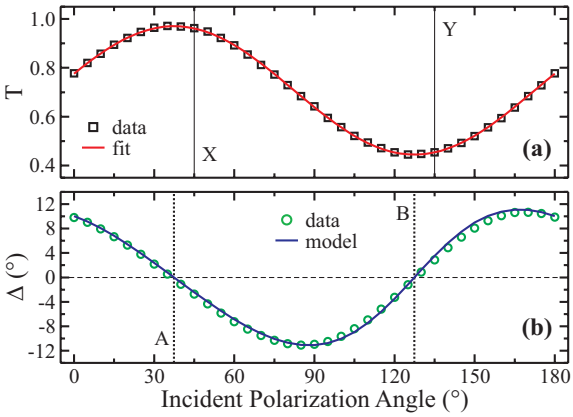

Fig. 2. (a) Transmittance ($\pm.01$) and fit to Eq. (1). Vertical lines indicate the axes X and Y. (b) Polarization azimuth rotation data ($\pm 0.1^\circ$) and model from Eq. (2). The vertical dotted lines indicate the axes A and B, while the horizontal dashed line is a zero-crossing guide to the eye.

Y by $\alpha = 45^\circ - \phi$. Of course, this model of the nanoparticles is naïve, but it does yield the correct shifts for the limiting cases of the symmetric L ($\alpha = 0^\circ$ for $\rho = 1$) and a vertical rod ($\alpha \Rightarrow 45^\circ$ for $\rho \gg 1$). (The model also holds for the converse situation, where the horizontal arm is longer than the vertical arm so that $\rho < 1$.) We therefore expect that for $\rho \simeq 1$, it should yield a reasonable approximation if the arm length difference is the dominant source of the axis shift. For $\rho = 1.05$, as in our particles, $\alpha \approx -1.5^\circ$, much smaller than the observed shift. The large discrepancy between the model and experimentally observed shift points towards a different source: other structural imperfections that strongly influence the optical response of the nanoparticles, which may include rounded corners, perimeter deviations, a possible height profile bias, and small-scale deformities that lead to local-field hot spots. Indeed, a measurement performed at 820 nm yields an even larger angular shift of -11.5° [17]. Higher multipole interactions likely may also be involved, but due to the complexity of incorporating them into this simple model, they have not yet been addressed in detail. A proper theoretical treatment of the optical responses would, of course, require full multipolar calculations.

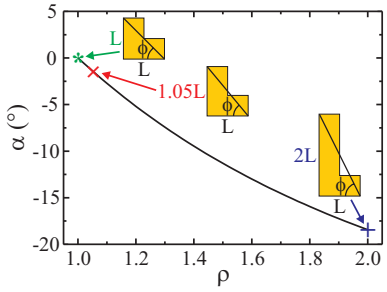

Fig. 3. Simple model to predict axis shift, α, based on the arm length ratio, ρ.

Regardless of other shape deviations, the lone fact that the arm lengths are different means that the symmetry of the particles is broken, so that the mirror plane along X no longer exists. The array should then be chiral and may exhibit optical activity, for which we checked by performing a polarization azimuth rotation measurement. For a given input linear polariza-

#5420 - $15.00 US
Received 1 October 2004; revised 19 October 2004; accepted 20 October 2004

tion direction, an analyzer was used to minimize the transmitted intensity, and the difference between the input and output directions, Δ, was calculated. Additionally, we can predict the expected rotation due to dichroism in our transmission model, Eq. (1) [17]:

$$\Delta = \arctan[\sqrt{\frac{T_B}{T_A}}\tan(\theta - 45^\circ - \alpha)] - (\theta - 45^\circ - \alpha). \quad (2)$$

Any deviation of the data from this model then implies effects other than dichroism, such as birefringence and/or optical activity. However, averaging over all incident polarization directions removes any contributions resulting from dichroism and birefringence [9]. In the absence of optical activity, this average should thus yield zero.

The model fits the data very well in Fig. 2(b), indicating that the observed rotation results essentially from dichroism. The computed average rotation is only -0.04°, while the zero crossings (the directions of zero azimuth rotation) are orthogonal and correspond to the A- and B-axes. These results together suggest that if the array is optically active at this wavelength, it is only weakly so, below the detection limit of the experiment. Interestingly, at 820 nm, measurable optical activity (0.3°) is observed [17].

However, the absence of measurable optical activity at a particular wavelength does not imply that the symmetry breaking is inconsequential. Second-order optical responses, SHG in particular, are highly sensitive to sample symmetry [18, 19] and are therefore better techniques for diagnosing broken symmetry. More specifically, we can measure the response of the in-plane components of the SHG tensor, $\chi^{(2)}_{ijk}(2\omega; \omega, \omega)$, where i, j, k, can be X, Y, or Z. According to the electric-dipole approximation, the mirror symmetry of the ideal array determines whether a particular input/output polarization combination allows a nonlinear response or is forbidden [19]. Because higher multipole contributions (electric-quadrupole or magnetic-dipole) obey the same selection rules, a non-zero forbidden signal then clearly reveals broken symmetry [20].

An ideal, symmetric, L-shaped nanoparticle belongs to the C_{1h} symmetry group, due to the substrate-air interfacial asymmetry. A regular array of ideal particles then exhibits the same symmetry properties, where reflection through the X-axis (Y $\rightarrow -$Y) is the sole non-trivial symmetry operation. Since our measurements are made at normal incidence, we will consider only the in-plane (XY) components. Accordingly, there are just four allowed components, of which only three are independent: XXX, XYY, and YXY = YYX. However, YXY and YYX are not individually accessible in our single-beam experiment due to the mixed nature of the input polarizations. There are two other directly accessible components that are forbidden: YXX and YYY (as are the inaccessible XXY = YXX). We therefore measured the responses for the four pure input/output polarization combinations XXX, XYY, YXX, and YYY. Because one may argue that A and B are the actual primary axes, we also measured the identical combinations with A replacing X and B replacing Y.

The results of Fig. 4 clearly indicate broken symmetry in our sample. While the forbidden crossed input/output responses YXX and BAA are zero, the forbidden parallel responses YYY and BBB are not only nonzero, they attain sizable fractions of the maximum responses, the crossed input/output combinations XYY and ABB. YYY is $\sim$ 10% of XYY (or, in terms of the susceptibility tensor, $\chi^{(2)}_{YYY} \sim 30\%\chi^{(2)}_{XYY}$). Since X-polarization (A-polarization) is not resonant for this array, the weak response from the allowed XXX (AAA) component is expected. However, the relatively large, non-zero forbidden signals show that the small imperfections in the nanoparticles strongly influence the optical responses of the array. Moreover, these results indicate that nonlinear measurements yield additional salient information about the broken symmetry, since an average polarization azimuth rotation was undetectable in the linear measurement.

#5420 - $15.00 US Received 1 October 2004; revised 19 October 2004; accepted 20 October 2004

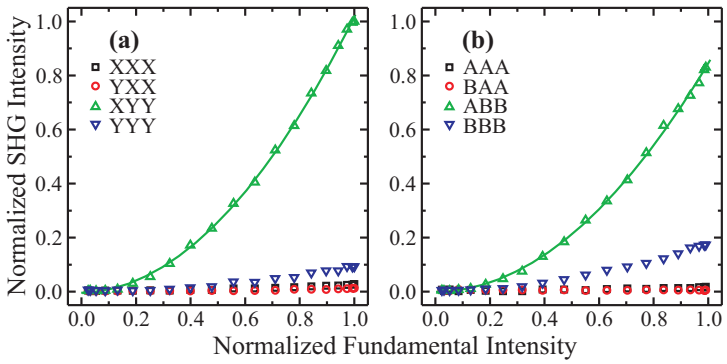

Fig. 4. Normalized SHG polarization responses for selected combinations of (a) XY polarizations and (b) AB polarizations (solid lines: quadratic fits).

4. Conclusion

Small structural deviations from the ideal shape existing in gold nanoparticles, such as arm length differences or edge protrusions, lead to large, unexpected linear and nonlinear optical responses. The primary extinction axes are shifted from their expected ideal-symmetry locations by a greater angle than simple geometrical considerations based on unequal arm lengths predict. The particles are highly sensitive to the state of polarization of the incident probe beam. Broken symmetry makes the particles, and hence the array, chiral, although measurable optical activity was not directly observed in the linear response at our laser wavelength. However, polarized second-harmonic generation measurements, being more sensitive to the lack of symmetry, reveal that responses forbidden to ideal, symmetric particles are not only present but are relatively large compared to the allowed response. While samples with more uniform particle shapes would be useful for establishing limits to the detection of effects due to broken symmetry, reproducibility issues hinder this prospect at present. Although metal nanoparticles may have many potential applications for nanoscale optical devices and components, these results show their high degree of polarization sensitivity and highlight the considerable effects of apparently minor deviations from assumed symmetry. Such significant influences require meticulous characterization in order to understand fully the optical responses of non-ideal nanoparticles.

Acknowledgments

We thank Y. P. Svirko, T. Vallius, and M. I. Stockman for insightful discussions. This work was funded by grants 102018 and 101362 from the Academy of Finland.

#5420 - $15.00 US Received 1 October 2004; revised 19 October 2004; accepted 20 October 2004